

**UNCLASSIFIED**

NAVAL AIR WARFARE CENTER AIRCRAFT DIVISION  
PATUXENT RIVER, MARYLAND



## REPORT OF TEST RESULTS

REPORT NO: NAWCADPAX--96-250-TR

COPY NO. 71

### LOAD RATIO DEPENDENCE OF FATIGUE THRESHOLD IN AERMET 100 STEEL

by

Eun U. Lee

2 October 1996

Aerospace Materials Division  
Air Vehicle and Crew Systems Technology Department  
Naval Air Warfare Center Aircraft Division  
Patuxent River, Maryland

19970220 012

Approved for public release; distribution is unlimited.

THIS QUALITY ASSURED

**UNCLASSIFIED**

DEPARTMENT OF THE NAVY  
NAVAL AIR WARFARE CENTER AIRCRAFT DIVISION  
PATUXENT RIVER, MARYLAND

NAWCADPAX--96-250-TR  
2 October 1996

**RELEASED BY:**

Wm Frazier 1/22/97  
WILLIAM E. FRAZIER / DATE  
Head, Metals and Ceramics Branch

Dale Moore 1/22/97  
DALE MOORE / DATE  
Director, Materials Competency  
Naval Air Warfare Center Aircraft Division

REPORT DOCUMENTATION PAGE			Form Approved OMB No. 0704-0188	
Public reporting burden for this collection of information is estimated to average 1 hour per response, including the time for reviewing instructions, searching existing data sources, gathering and maintaining the data needed, and completing and reviewing the collection of information. Send comments regarding this burden estimate or any other aspect of this collection of information, including suggestions for reducing this burden, to Washington Headquarters Services, Directorate for Information Operations and Reports, 1215 Jefferson Davis Highway, Suite 1204, Arlington, VA 22202-4302, and to the Office of Management and Budget, Paperwork Reduction Project (0704-0188), Washington, DC 20503.				
1. AGENCY USE ONLY (Leave Blank)	2. REPORT DATE 2 October 1996	3. REPORT TYPE AND DATES COVERED		
4. TITLE AND SUBTITLE  Load Ratio Dependence of Fatigue Threshold in AerMet 100 Steel		5. FUNDING NUMBERS		
6. AUTHOR(S)  Eun U. Lee				
7. PERFORMING ORGANIZATION NAMES(S) AND ADDRESS(ES)  Naval Air Warfare Center Aircraft Division 22347 Cedar Point Road Unit #6 Patuxent River, Maryland 20670-1161		8. PERFORMING ORGANIZATION REPORT NUMBER  NAWCADPAX--96-250-TR		
9. SPONSORING / MONITORING AGENCY NAME(S) AND ADDRESS(ES)  Naval Air Systems Command 1421 Jefferson Davis Highway Arlington, Virginia 22243		10. SPONSORING / MONITORING AGENCY REPORT NUMBER		
11. SUPPLEMENTARY NOTES				
12a. DISTRIBUTION / AVAILABILITY STATEMENT  Approved for public release; distribution is unlimited.			12b. DISTRIBUTION CODE	
13. ABSTRACT (Maximum 200 words)  A study was conducted on the fatigue crack growth behavior of AerMet 100 steel at various load ratios in a gaseous dry nitrogen environment. Increasing the load ratio increased the near-threshold fatigue crack growth rate and reduced the threshold stress intensity range for fatigue crack growth, $\Delta K_{th}$ . $\Delta K_{th}$ decreased with increasing load ratio up to a critical value, $R_{cr} = 0.5$ , and then leveled off. The maximum stress intensity at threshold, $K_{max}$ , changed little below $R_{cr}$ but increased rapidly above $R_{cr}$ . The critical threshold stress intensity range, $\Delta K_{th}^*$ , and the critical maximum stress intensity, $K_{max}^*$ , were determined to be 2.22 and 3.42 MPa $\sqrt{m}$ , respectively. The fatigue crack growth behavior changed from Class-IIb to Class-IIa with increasing fatigue crack growth rate.				
14. SUBJECT TERMS Fatigue Crack Growth      Tensile Strength Threshold Stress Intensity      Load Ratio Maximum Stress Intensity			15. NUMBER OF PAGES 23	
			16. PRICE CODE	
17. SECURITY CLASSIFICATION OF REPORT  UNCLASSIFIED	18. SECURITY CLASSIFICATION OF THIS PAGE  UNCLASSIFIED	19. SECURITY CLASSIFICATION OF ABSTRACT  UNCLASSIFIED	20. LIMITATION OF ABSTRACT  SAR	

NSN 7540-01-280-5500

Standard Form 298 (Rev. 2-89)  
Prescribed by ANSI Std. Z39-18  
298-102

### ABSTRACT

A study was conducted on the fatigue crack growth behavior of AerMet 100 steel at various load ratios in a gaseous dry nitrogen environment. Increasing the load ratio increased the near-threshold fatigue crack growth rate and reduced the threshold stress intensity range for fatigue crack growth,  $\Delta K_{th}$ .  $\Delta K_{th}$  decreased with increasing load ratio up to a critical value,  $R_{cr} = 0.5$ , and then leveled off. The maximum stress intensity at threshold,  $K_{max}$ , changed little below  $R_{cr}$  but increased rapidly above  $R_{cr}$ . The critical threshold stress intensity range,  $\Delta K_{th}^*$ , and the critical maximum stress intensity,  $K_{max}^*$ , were determined to be 2.22 and 3.42 MPa $\sqrt{m}$ , respectively. The fatigue crack growth behavior changed from Class-IIb to Class-IIa with increasing fatigue crack growth rate.

### ACKNOWLEDGMENT

*This study was supported by the ONR 6.2 Exploratory Development Program in Airborne Structural Materials, PE 62234N.*

## CONTENTS

	<u>Page No.</u>
ABSTRACT .....	ii
ACKNOWLEDGMENT .....	ii
SUMMARY .....	1
INTRODUCTION .....	1
EXPERIMENTAL PROCEDURE .....	1
RESULTS AND DISCUSSION .....	3
FATIGUE CRACK GROWTH RATE AND STRESS INTENSITY RANGE.....	3
THRESHOLD STRESS INTENSITY RANGE AND MAXIMUM .....	3
STRESS INTENSITY	
CONCLUSIONS.....	5
REFERENCES .....	7
APPENDIX	
A. FIGURES .....	9
DISTRIBUTION.....	18

## SUMMARY

The fatigue crack growth (FCG) behavior of AerMet 100 steel was investigated at various load ratios, ranging from 0.05 to 0.9, in gaseous dry nitrogen. The results of this investigation can be summarized as follows.

Raising the load ratio increases the near-threshold FCG rate below  $10^{-5}$  mm/cycle and reduces the threshold stress intensity range,  $\Delta K_{th}$ . However, such an effect of load ratio on FCG rate is little above  $10^{-5}$  mm/cycle.  $\Delta K_{th}$  decreases with increasing load ratio up to the critical value,  $R_{cr} = 0.5$ , and levels off above the  $R_{cr}$ . With an increase in load ratio, the maximum stress intensity at threshold,  $K_{max}$ , increases little from its critical value at load ratio 0. However, it increases rapidly above the  $R_{cr}$ . The critical threshold stress intensity range,  $\Delta K_{th}^*$ , is 2.22 MPa $\sqrt{m}$  and the critical maximum stress intensity at threshold,  $K_{max}^*$ , 3.42 MPa $\sqrt{m}$ . The FCG behavior of AerMet 100 steel changes from Class-IIb to Class-IIa with increasing  $da/dN$  in dry gaseous nitrogen. The resistance of AerMet 100 steel to threshold fatigue crack growth is determined to be similar to that of 4340 and 300M steels.

## INTRODUCTION

Advanced aircraft landing gear and other components demand strong and tough materials to achieve higher performance and greater reliability. In the past, 300M and AF1410 steels were accepted as the materials for aircraft landing gear because of the high strength (300M) and the great fracture toughness (AF1410). Recently, a new Co-Ni alloy steel, strengthened with carbon, chromium, and molybdenum, AerMet 100, was developed. This steel has an outstanding combination of high ultimate tensile strength (UTS), 1,930 - 2,070 MPa, and high fracture toughness,  $K_{IC}$ , exceeding 120 MPa $\sqrt{m}$ . The UTS and  $K_{IC}$  are similar to and much greater than those of 300M steel, 2,000 MPa and 65 MPa $\sqrt{m}$ , respectively. On the one hand, they are greater and less than those of AF1410 steel, 1,585-1,724 MPa and 165 MPa $\sqrt{m}$ , respectively. Therefore, AerMet 100 steel can replace 300M steel to increase damage tolerance and AF1410 steel to achieve weight reduction. This suggests that AerMet 100 steel has a great potential for application to fracture resistant components, including aircraft landing gear. However, the FCG behavior of this steel was not fully understood.

The objective of this study was to investigate the FCG behavior of AerMet 100 steel, with special emphasis on near-threshold crack growth at different load ratios. A series of fatigue tests were conducted with a frequency of 10 Hz at various load ratios, ranging from 0.05 to 0.9, in gaseous dry nitrogen environment, employing C-R oriented specimens of AerMet 100 steel.

## EXPERIMENTAL PROCEDURE

The specimen material, an AerMet 100 steel forging, was supplied by Carpenter Technology Corp. in the form of a 108 mm diameter round bar. The chemical composition of this steel is given in table 1.

Table 1  
CHEMICAL COMPOSITION OF AERMET 100 STEEL BAR

Element	Weight (%)
C	0.23
Mn	0.03
Si	0.03
P	0.003
S	0.0009
Cr	3.03
Ni	11.09
Mo	1.18
Cu	0.01
Co	13.44
Al	0.005
Ti	0.009
Fe	bal

The test specimen, selected for this study, was a C-R oriented compact-tension (C(T)) specimen with a width of 25.4 mm and a thickness of 6.35 mm. Specimen blanks, slightly larger than the finished specimen, were removed from the 108 mm diameter bar forging and subjected to the following heat treatment: solution treatment at 885°C for 1 hr, oil quenching to room temperature, refrigeration in liquid nitrogen for 1 hr, and aging at 482°C for 5 hr. The resultant UTS and yield strength were 1,965 and 1,724 MPa, respectively. The plane strain fracture toughness,  $K_{IC}$ , was 126 MPa $\sqrt{m}$ . The C(T) specimens were prepared by electro discharge machining to the final dimension.

FCG tests were conducted on a 445 kN closed-loop servo-hydraulic Materials Testing System (MTS) machine, monitored and controlled by a computer. The MTS machine was operated under constant amplitude sine wave loading at a frequency of 10 Hz and load ratios ( $R$  = minimum load/maximum load), ranging from 0.05 to 0.9. The loading was carried out in a Plexiglas environmental chamber, which was filled with gaseous dry nitrogen and an enclosed specimen. Oil free gaseous nitrogen was dried to 5% relative humidity by passing through Drierite (CaSO<sub>4</sub>) prior to entering the environmental chamber. The crack length was continuously monitored by compliance measurement technique. The precision of this crack length measurement technique was typically 0.025 mm. Near-threshold crack growth rates were obtained under decreasing  $K$  (load shedding) condition with  $K$ -gradient parameter  $C = -0.16 \text{ mm}^{-1}$ .

## RESULTS AND DISCUSSION

### FATIGUE CRACK GROWTH RATE AND STRESS INTENSITY RANGE

The variation of FCG rate,  $da/dN$ , with stress intensity range,  $\Delta K$ , is shown in figures A-1, A-2, and A-3 for  $R = 0.05$  to  $0.9$ . Raising  $R$  increases the near-threshold FCG rate below  $10^{-5}$  mm/cycle and reduces the threshold stress intensity range,  $\Delta K_{th}$ . However, near and above  $10^{-5}$  mm/cycle, the curves of  $da/dN$  versus  $\Delta K$  tend to converge, indicating diminishing  $R$  effect with increasing  $da/dN$ . This behavior has also been observed in various steels and other materials by a number of investigators.<sup>1-21</sup> Some investigators attributed this behavior in steels to crack closure, induced by plasticity, oxide, or/and surface roughness.<sup>1-9</sup>

### THRESHOLD STRESS INTENSITY RANGE AND MAXIMUM STRESS INTENSITY

The variations of threshold stress intensity range,  $\Delta K_{th}$ , and maximum stress intensity,  $K_{max} = \Delta K_{th} / (1-R)$ , with  $R$  are shown in figure A-4.  $\Delta K_{th}$  decreases with increasing  $R$  until  $R$  reaches a critical value,  $R_{cr} = 0.5$ . At  $R > 0.5$ ,  $\Delta K_{th}$  levels off and is relatively constant. As  $R$  approaches 1,  $\Delta K_{th}$  reaches a critical value,  $\Delta K_{th}^* = 2.22 \text{ MPa}\sqrt{\text{m}}$ . With an increase in  $R$ ,  $K_{max}$  increases very little from the critical value at  $R = 0$ . The critical value at  $R = 0$  is  $K_{max}^* = 3.42 \text{ MPa}\sqrt{\text{m}}$ . However, above  $R_{cr}$ ,  $K_{max}$  increases steeply with  $R$ , maintaining  $\Delta K_{th}$  constant. The two critical stress intensity parameters  $\Delta K_{th}^*$  and  $K_{max}^*$  are known to be affected by microstructure and environment.<sup>20</sup> The dependence of  $\Delta K_{th}$  and  $K_{max}$  on  $R$  can be described in terms of the  $\Delta K_{th}^*$  and  $K_{max}^*$ . For  $R < R_{cr}$ ,  $\Delta K_{th} = K_{max}^* (1-R)$  and  $K_{max} = K_{max}^*$ , and for  $R > R_{cr}$ ,  $\Delta K_{th} = \Delta K_{th}^*$  and  $K_{max} = \Delta K_{th}^* / (1-R)$  and  $R_{cr} = 1 - (\Delta K_{th}^* / K_{max}^*)$ .

Using the  $\Delta K_{th}$ - $R$  data, the entire FCG behavior may be divided into five different classes, as shown schematically in figure A-5.<sup>21</sup> This classification helps in recognizing the individual fatigue behavior of a different family of materials and understanding the relative roles of the environment on fatigue. Class-V behavior is observable in polymeric materials but seldom in metals. The  $\Delta K_{th}$  increases with  $R$ . Class-I behavior, where  $\Delta K_{th}$  is independent of  $R$ , is seen in aluminum-, nickel-, and titanium-alloys and some steels. This trend pertains to materials that are insensitive to environmental effects, commonly observed in vacuum. In the Class-II behavior,  $\Delta K_{th}$  versus  $R$  extrapolates to an intercept of  $\Delta K_{th} > 1$  at  $R = 1$ . This behavior is noticeable in pure materials of low strength and high ductility and in some of medium/high strength steels having high fracture toughness.<sup>21,22</sup> The Class-II is subdivided further into Class-IIa and Class-IIb. Class-III is a normal fatigue behavior, commonly observed in aluminum alloys and some steels. Here  $\Delta K_{th}$  versus  $R$  curve extrapolates to  $R = 1$  at  $\Delta K_{th} = 0$ . Class-IV shows the behavior with  $\Delta K_{th} < 1$  at  $R = 1$ . Class-IV is also subdivided into Class-IVa and Class-IVb. According to this classification, the fatigue behavior of AerMet 100 steel in gaseous dry nitrogen is Class-II.

$\Delta K_{th}$  is plotted against  $K_{max}$ , determined from  $K_{max} = \Delta K_{th} / (1-R)$ , for AerMet 100 in figure A-6. Such a plot, called fundamental threshold curve, provides interrelation between the two parameters  $\Delta K_{th}$  and  $K_{max}$  defining regimes, where fatigue crack grows (above the curve) and



where it does not (below the curve).<sup>21</sup> In other words, the curve delineates a boundary where FCG starts for a given  $K_{\max}$  and indicates the resistance to threshold FCG. The figure A-6 also includes limited data of  $\Delta K_{\text{th}}$  versus  $K_{\max}$  for 4340<sup>9</sup> and 300M<sup>12</sup> steels. From this figure, AerMet 100, 4340, and 300M steels appear to have similar resistance to threshold fatigue crack growth, though their fracture toughnesses are different. (The  $K_{\text{IC}}$  values are 120, 53, and 65 MPa $\sqrt{\text{m}}$  for AerMet 100, 4340, and 300M steels, respectively.)

The variations of  $\Delta K$  with  $R$  and  $K_{\max}$  are shown for various FCG rates, ranging from  $1 \times 10^{-8}$  to  $1 \times 10^{-5}$  mm/cycle, in figures A-7 and A-8, respectively. The  $\Delta K$  versus  $R$  curve has a negative slope with a positive intercept at  $R = 1$ , and a plateau is observable in the curve only at lower FCG rates, figure A-7. The curvatures of the  $\Delta K$  versus  $K_{\max}$  (or fundamental threshold) curves in figure A-8 are large. The large curvature is characteristic of Class-II behavior and indicative of an interaction between  $\Delta K$  and  $K_{\max}$ .<sup>21</sup> Such features signify a transition of FCG behavior from Class-IIb to Class-IIa with increasing  $da/dN$ .

## CONCLUSIONS

Raising load ratio  $R$  increases the near-threshold FCG rate below  $10^{-5}$  mm/cycle and reduces the threshold stress intensity range  $\Delta K_{th}$  in gaseous dry nitrogen. However, such an effect of  $R$  on FCG rate is little above  $10^{-5}$  mm/cycle.

$\Delta K_{th}$  decreases with increasing  $R$  up to the critical value,  $R_{cr} = 0.5$ , and then levels off above the  $R_{cr}$  in gaseous dry nitrogen. With an increase in  $R$ , the threshold maximum stress intensity,  $K_{max}$ , increases little from its critical value at  $R = 0$ . However, it increases steeply above the  $R_{cr}$ . The critical threshold stress intensity range,  $\Delta K_{th}^*$ , and the critical threshold maximum stress intensity,  $\Delta K_{max}^*$ , are 2.22 and 3.42  $\text{Mpa}\sqrt{\text{m}}$ , respectively.

The FCG behavior of AerMet 100 steel in gaseous dry nitrogen is Class-II and changes from Class-IIb to Class-IIa with increasing  $da/dN$ .

The resistance of AerMet 100 steel to threshold fatigue crack growth is similar to that of 4340 and 300M steels.

THIS PAGE INTENTIONALLY LEFT BLANK

## REFERENCES

1. R. A. Schmidt and P. C. Paris: Progress in Flaw Growth and Fracture Toughness Testing, ASTM STP 536, American Society for Testing and Materials, Philadelphia, PA, 1973, pp. 79-94.
2. R. O. Ritchie, S. Suresh, and C. M. Moss: Journal of Engineering Materials and Technology, ASME Trans., 1980, Vol. 102, pp. 293-299.
3. A. T. Stewart: Engineering Fracture Mechanics, 1980, Vol. 13, pp. 463-478.
4. S. Suresh, G. F. Zamiski, and R. O. Ritchie: Metall. Trans. A, 1981, Vol. 12A, pp. 1435-1443.
5. Y. Nakai, K. Tanaka, and T. Nakanishi: Engineering Fracture Mechanics, 1981, Vol. 15, pp. 291-302.
6. A. F. Blom: Fatigue Crack Growth Threshold Concepts, Eds. D. L. Davidson and S. Suresh, The Metallurgical Society of AIME, 1984, pp. 263-279.
7. G. T. Gray, III, J. C. Williams, and A. W. Thompson: Metall. Trans. A, 1983, Vol. 14A, pp. 421-433.
8. P. K. Liaw, A. Saxena, V. P. Swaminathan, and T. T. Shih: Fatigue Crack Growth Threshold Concepts, Eds. D. L. Davidson and S. Suresh, The Metallurgical Society of AIME, 1984, pp. 205-223.
9. P. K. Liaw, T. R. Leax, and J. K. Donald: Acta Metall, 1987, Vol. 35, pp. 1415-1432.
10. A. J. Cadman, C. E. Nicholson, and R. Brook: Fatigue Crack Growth Threshold Concepts, Eds. D. L. Davidson and S. Suresh, The Metallurgical Society of AIME, 1984, pp. 281-298.
11. K. A. Esaklul, A. G. Wright, and W. W. Gerberich: Fatigue Crack Growth Threshold Concepts, Eds. D. L. Davidson and S. Suresh, The Metallurgical Society of AIME, 1984, pp. 299-326.
12. R. O. Ritchie: Journal of Engineering Materials and Technology, 1977, pp. 195-204.
13. R. O. Ritchie: International Metals Reviews, 1979, Nos. 5 and 6, pp. 205-230.
14. B. R. Kirby and C. J. Beevers: Fatigue of Engineering Materials & Structures, 1979, Vol. 1, pp. 203-215.
15. H. Doker and G. Marci: International Journal of Fatigue, 1983, Vol. 5, pp. 187-191.

16. M. C. Lafarie-Frenot and C. Gasc: *Fat. Engng. Matl. Struct.*, 1983, Vol. 6, pp. 329-344.
17. S. Suresh, A. K. Vasudevan, and P. E. Bretz: *Metall. Trans. A*, 1984, Vol. 15A, pp. 369-379.
18. L. X. Han and S. Suresh: *Journal of American Ceramic Society*, 1989, Vol. 72, pp. 1233-1238.
19. A. K. Vasudevan and K. Sadananda: *Scripta Metall. et Materialia.*, 1993, Vol. 28, pp. 837-842.
20. A. K. Vasudevan, K. Sadananda, and N. Louat: *Scripta Metall. et Materialia*, 1993, Vol. 28, pp. 65-70.
21. A. K. Vasudevan and K. Sadananda: *Metall. Mater. Trans. A*, 1995, Vol. 26A, pp. 1221-34.
22. A. K. Vasudevan and K. Sadananda: *Proceedings of the 10th Biennial European Conference on Fracture - ECF 10, Berlin, Germany, 20-23 Sep 1994, Structural Integrity: Experiments - Models - Applications*, Eds. K-H. Schwalbe and C. Berger, Engineering Advisory Services Ltd., West Midlands, U. K., Vol. II, 1995.

APPENDIX A  
FIGURES

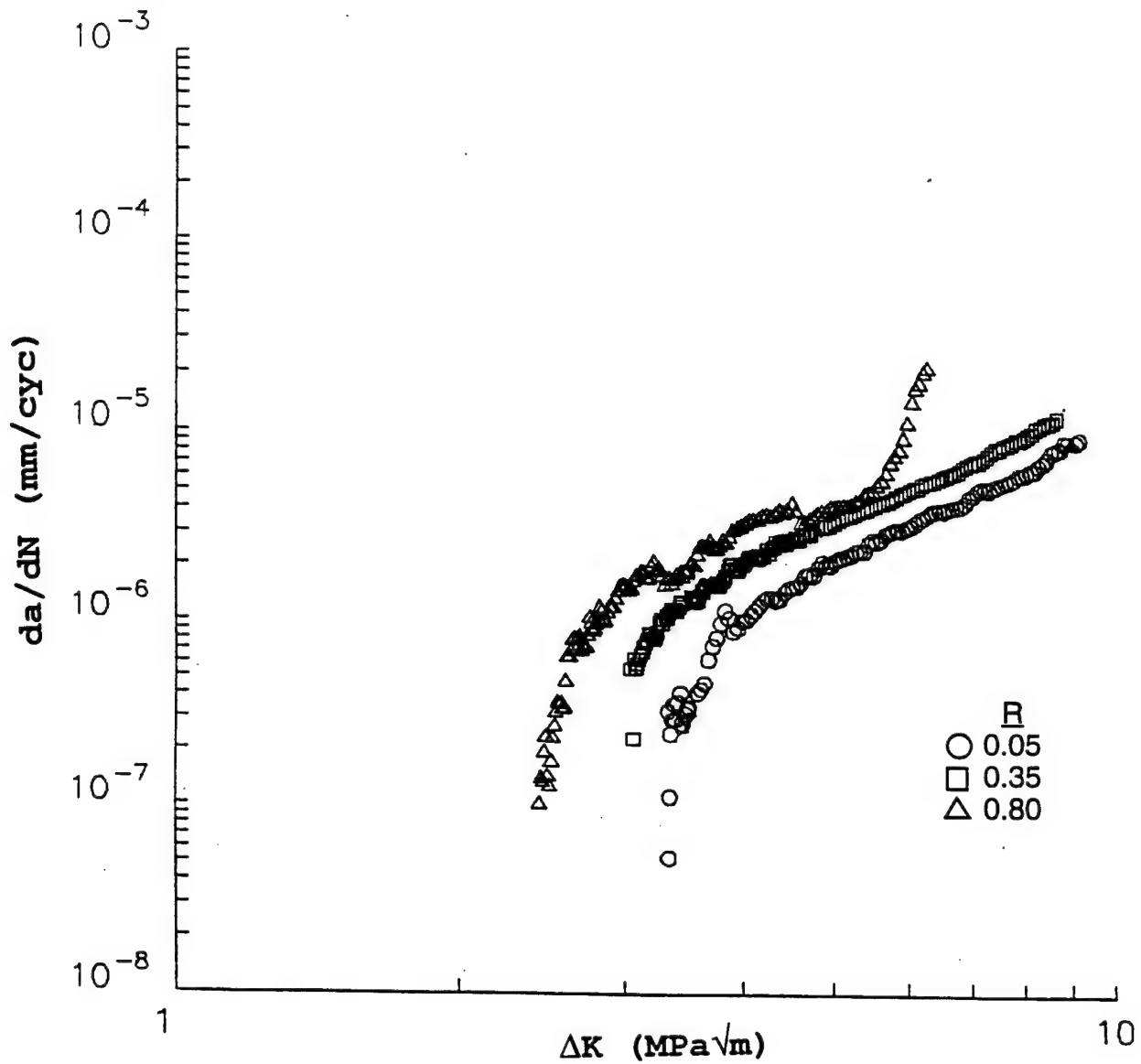


Figure A-1  
VARIATION OF FATIGUE CRACK GROWTH RATE,  $da/dN$ , WITH  
STRESS INTENSITY RANGE,  $\Delta K$ , AT LOAD RATIO  $R = 0.05, 0.35$ , AND  $0.8$

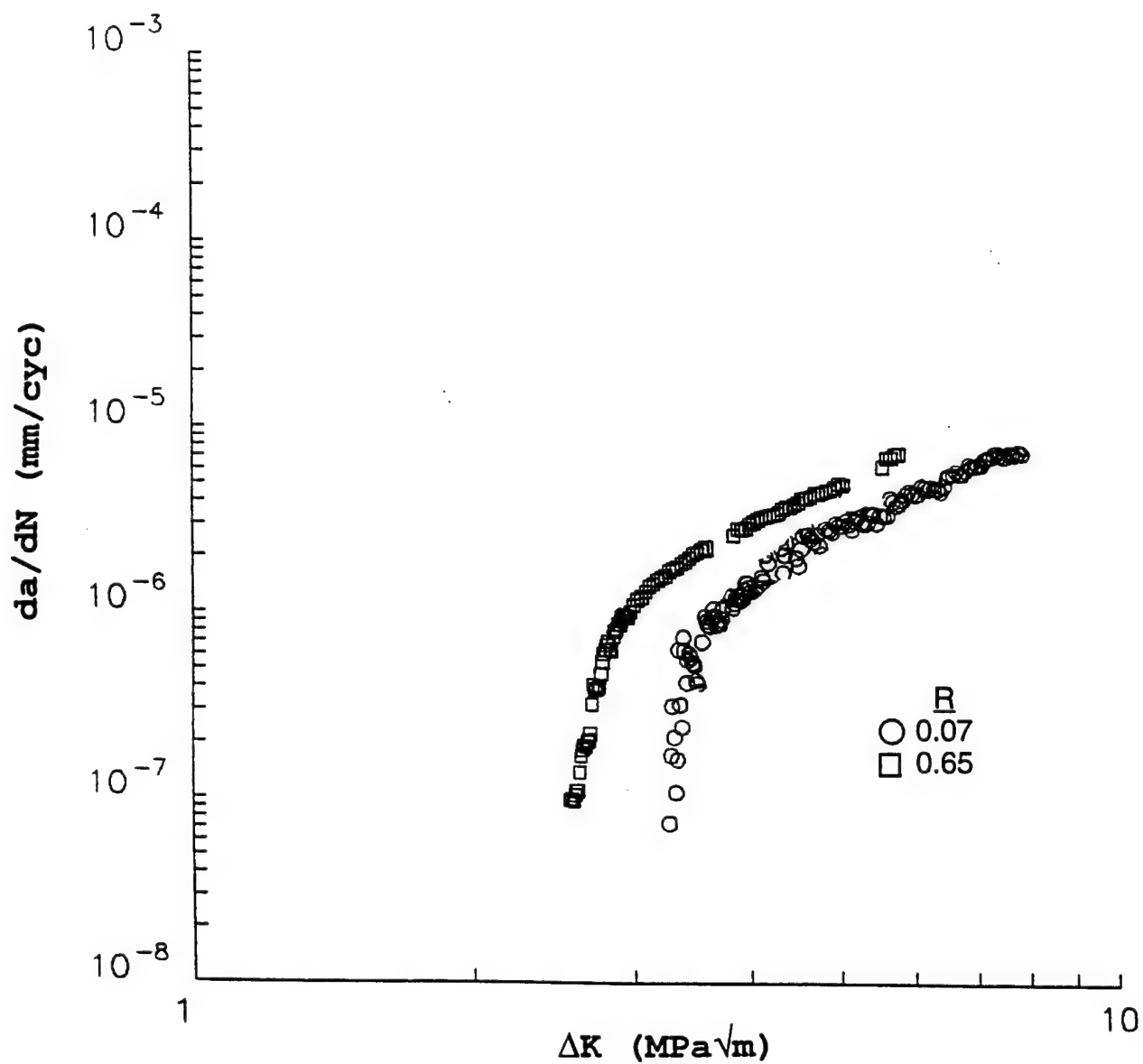


Figure A-2  
VARIATION OF FATIGUE CRACK GROWTH RATE,  $da/dN$ , WITH  
STRESS INTENSITY RANGE,  $\Delta K$ , AT LOAD RATIO  $R = 0.07$  AND  $0.65$



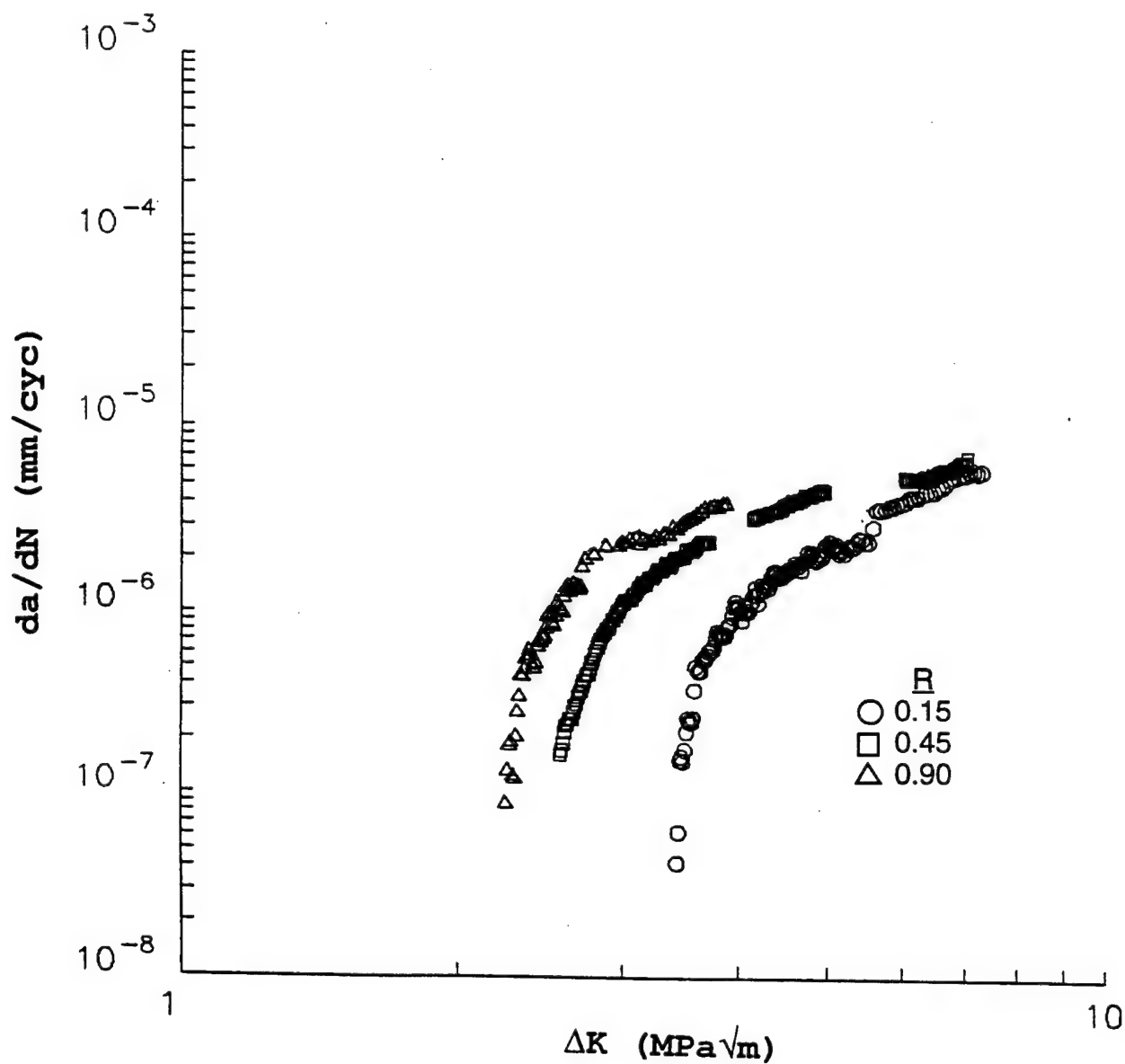


Figure A-3  
VARIATION OF FATIGUE CRACK GROWTH RATE,  $da/dN$ , WITH  
STRESS INTENSITY RANGE,  $\Delta K$ , AT LOAD RATIO  $R = 0.15, 0.45$ , AND  $0.9$

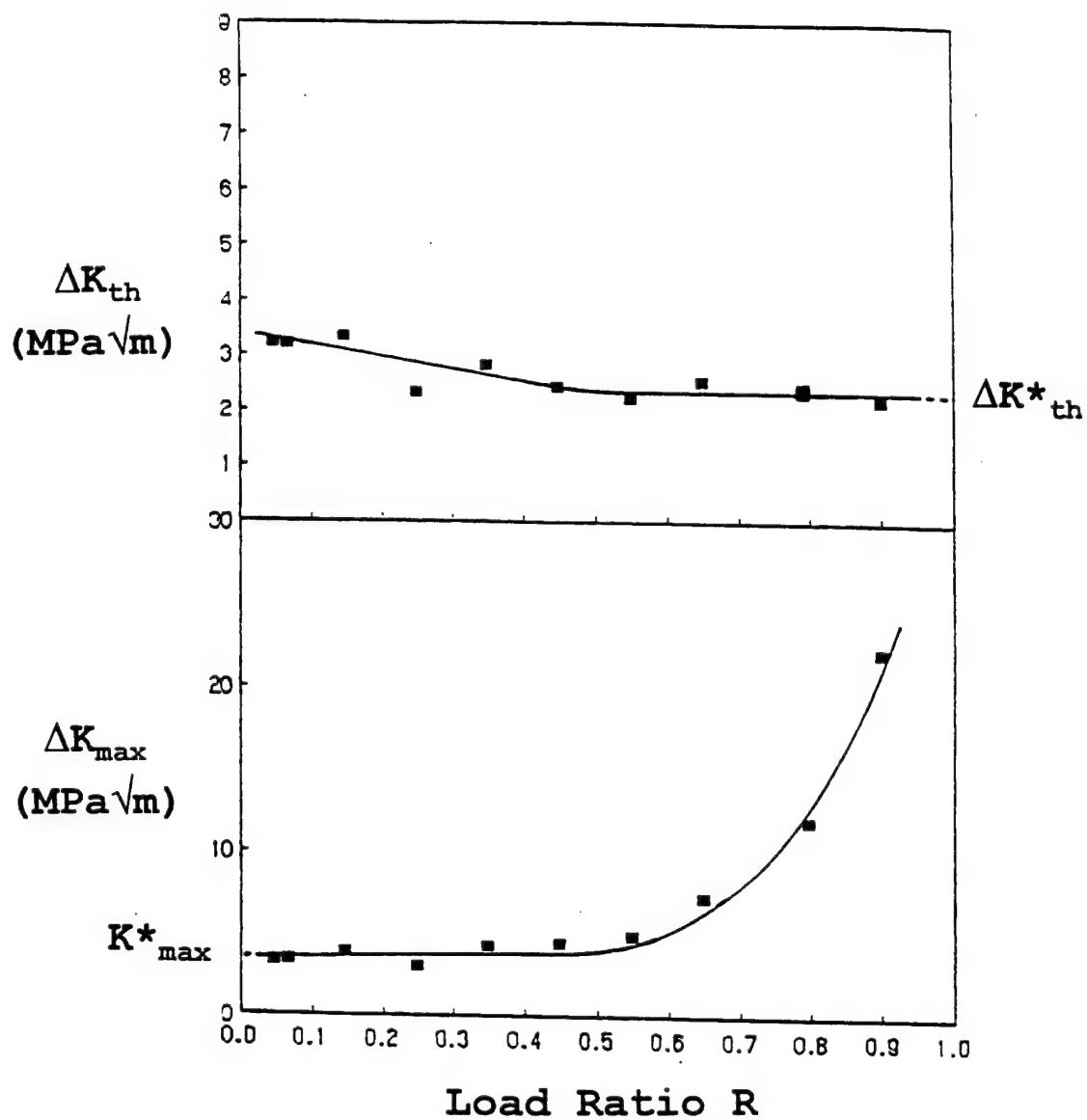


Figure A-4  
 VARIATION OF ALTERNATING AND MAXIMUM STRESS INTENSITIES  
 AT THRESHOLD,  $\Delta K_{th}$  AND  $K^*_{max}$ , WITH LOAD RATIO R

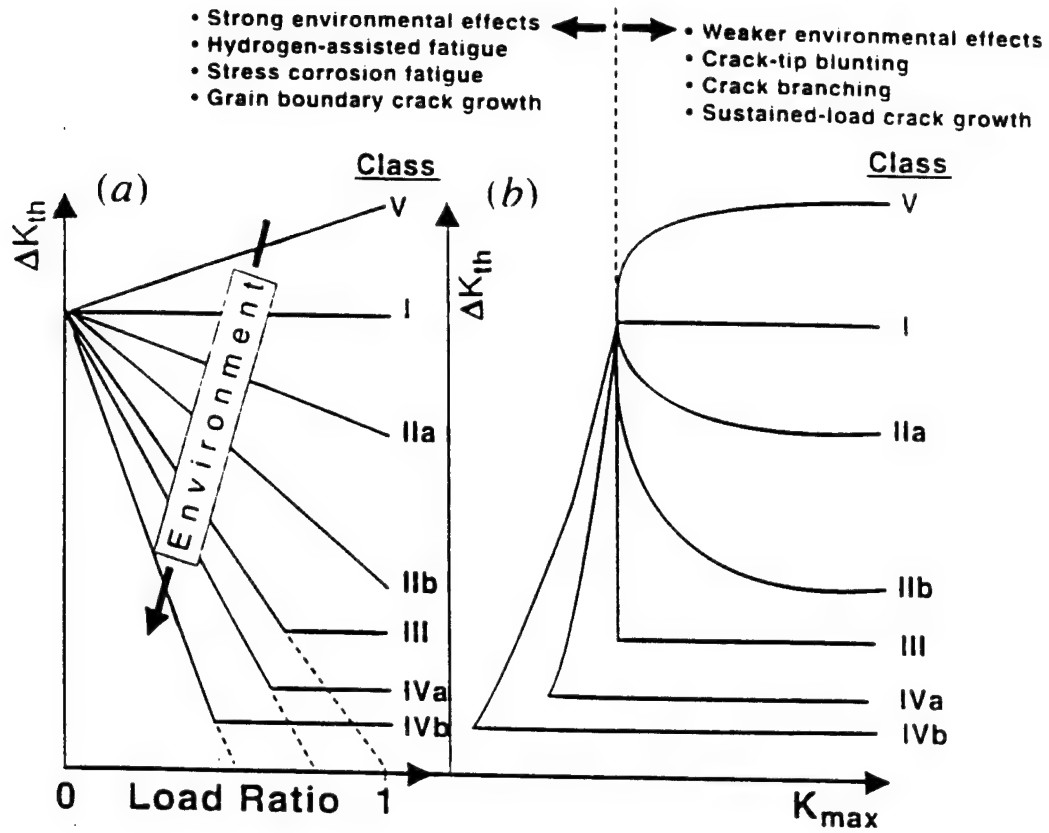


Figure A-5  
CLASSIFICATION OF FATIGUE CRACK GROWTH BEHAVIOR<sup>21</sup>

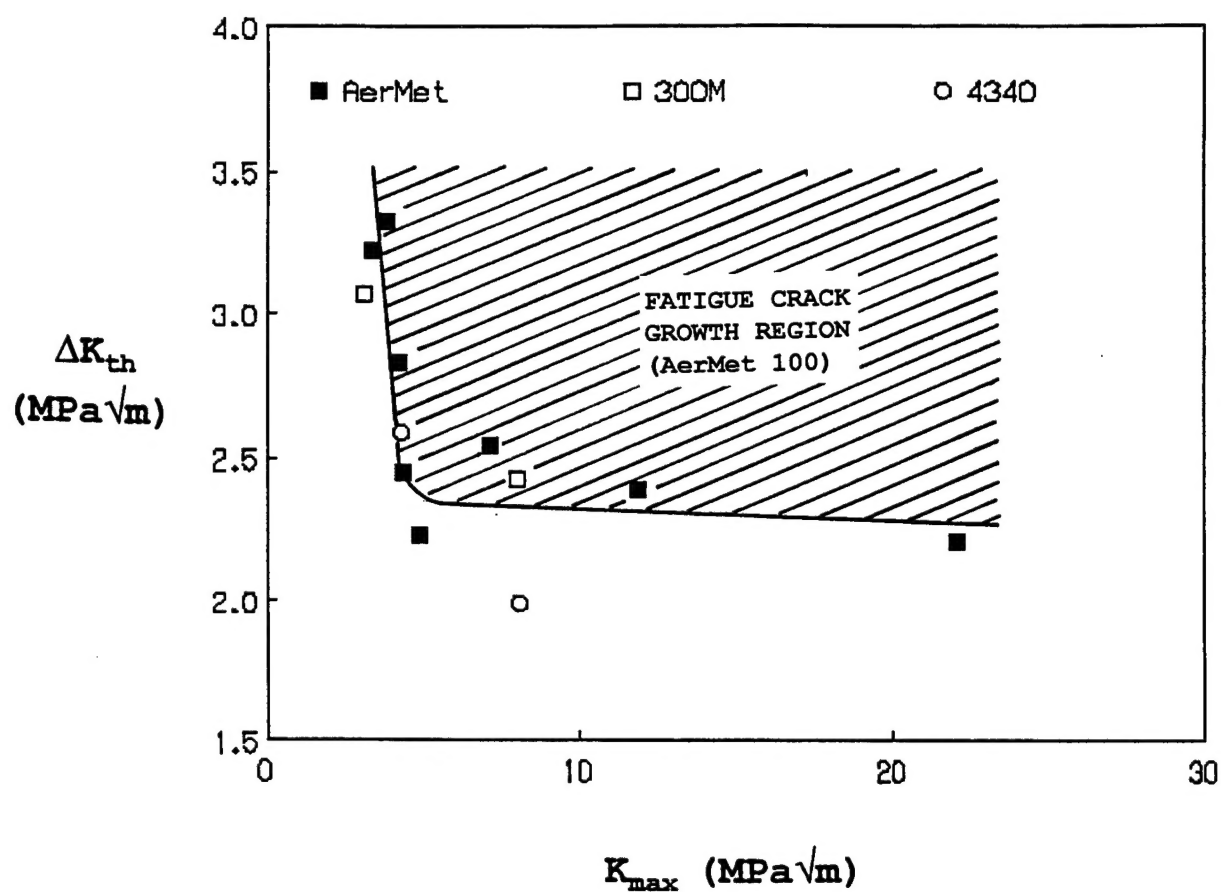


Figure A-6  
VARIATION OF  $\Delta K_{th}$  WITH  $K_{max}$   
(Fundamental Threshold Curve)

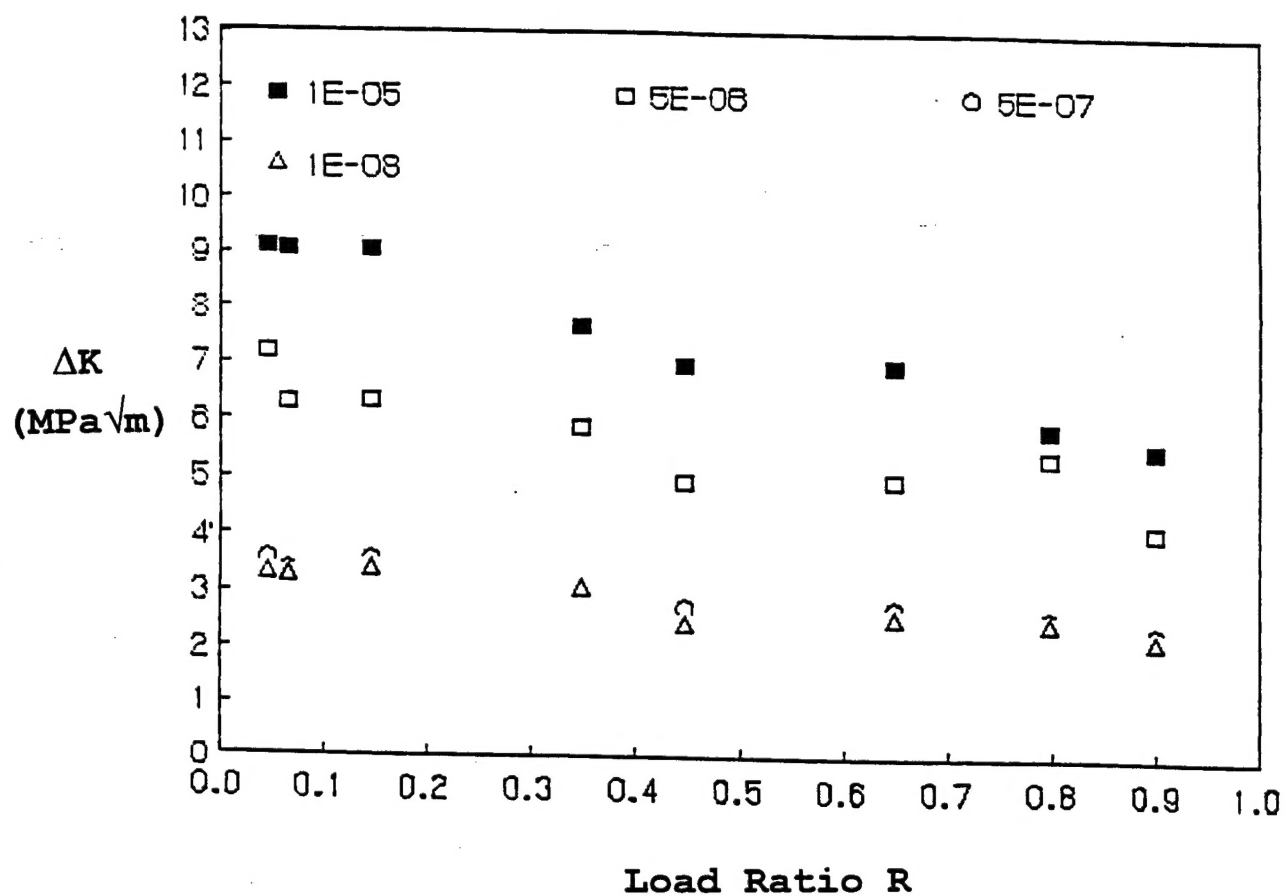


Figure A-7  
VARIATION OF  $\Delta K$  AT VARIOUS  $da/dN$  LEVELS VARIATION WITH  $R$

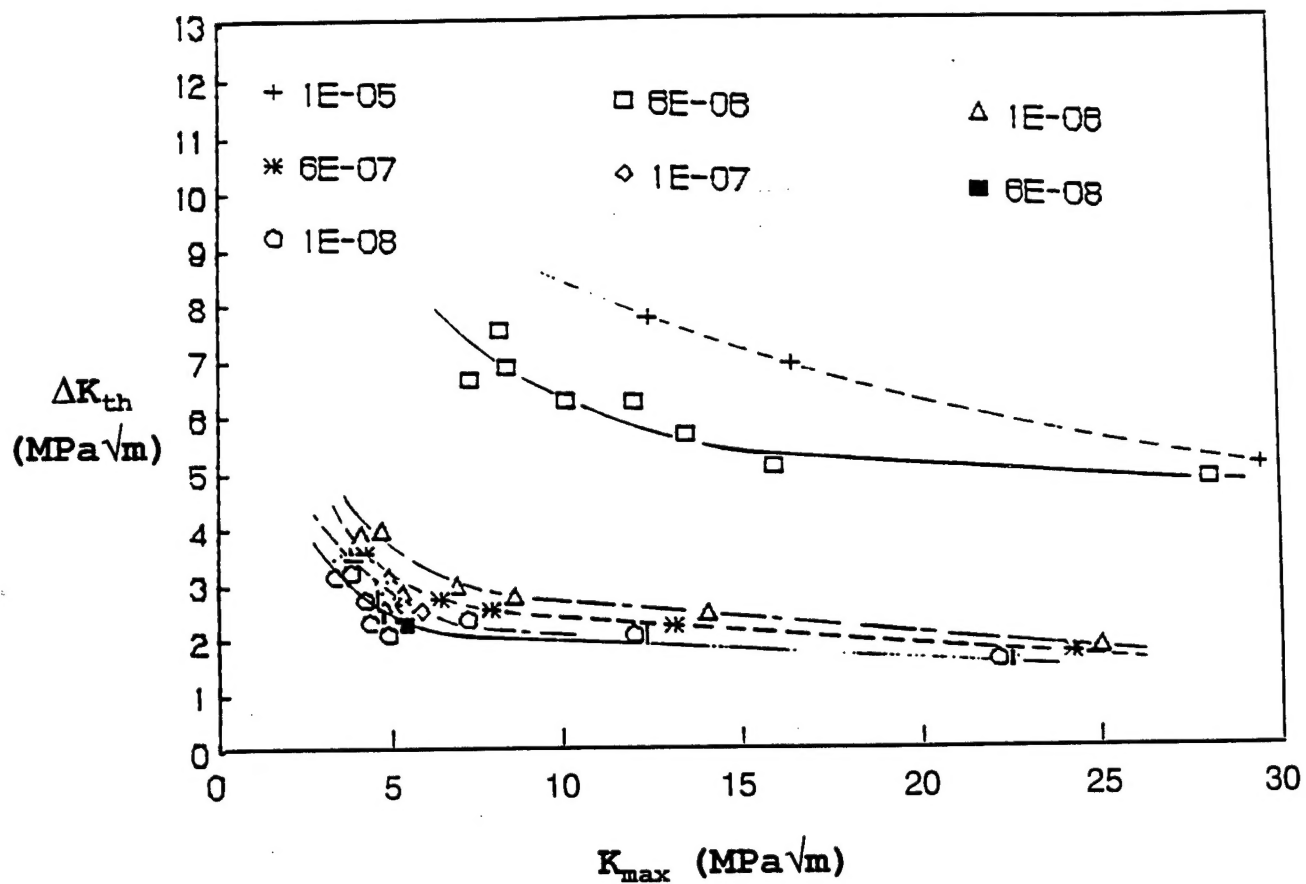


Figure A-8  
VARIATION OF  $\Delta K$  AT VARIOUS  $da/dN$  LEVELS VARIATION WITH  $K_{max}$

DISTRIBUTION:

Army Materials Command (AMCCE-BD)	(1)
JSF, Suite 307, 1745 Jefferson-Davis Highway, Arlington, VA 22202	(1)
NADEP Cherry Point, NC (4.3.4)	(1)
NADEP Jacksonville, FL (4.3.4)	(1)
NADEP San Diego, CA (4.3.4)	(1)
NAVAIRSYSCOM Washington, DC (AIR-4.1.1)	(1)
NAVAIRSYSCOM Washington, DC (AIR-4.3.2)	(1)
NAVSEASYSYSCOM Washington, DC	(5)
NRL Washington, DC	(2)
Carpenter Technology Corp.	(1)
Reading, PA	
NAVAIRWARCENACDIV Lakehurst, NJ	(1)
NAVAIRWARCENACDIV Patuxent River, MD (4.3.4.2)	(50)
NAVAIRWARCENACDIV Patuxent River, MD (4.4)	(2)
NAVAIRWARCENACDIV Patuxent River, MD (Technical Publishing Team)	(2)
DTIC	(1)